

Anomalous fluctuations of vertical velocity of Earth and their possible implications for earthquakes

Pouya Manshour,¹ Fatemeh Ghasemi,² T. Matsumoto,^{3,4} J. Gómez,⁵ Muhammad Sahimi,^{2,*} J. Peinke,⁶
A. F. Pacheco,⁷ and M. Reza Rahimi Tabar^{1,4,6,8}

¹*Department of Physics, Sharif University of Technology, Tehran 11155-9161, Iran*

²*Mork Family Department of Chemical Engineering and Materials Science, University of Southern California, Los Angeles, California 90089-1211, USA*

³*Division of Physics and Astronomy, Graduate School of Science, Kyoto University, Kitashirakawa Oiwakecho, Sakyo-ku, Kyoto 606-8502, Japan*

⁴*CNRS UMR 6202, Observatoire de la Côte d'Azur, BP 4229, 06304 Nice Cedex 4, France*

⁵*Earth Sciences Department, University of Zaragoza, Zaragoza 50009, Spain*

⁶*Institute of Physics, Carl von Ossietzky University, D-26111 Oldenburg, Germany*

⁷*Department of Theoretical Physics, University of Zaragoza, Pedro Cerbuna 12, 50009 Zaragoza, Spain*

⁸*Fachbereich Physik, Universität Osnabrück, Barbarastrasse, 49706 Osnabrück, Germany*

(Received 23 November 2009; revised manuscript received 9 February 2010; published 8 September 2010)

High-quality measurements of seismic activities around the world provide a wealth of data and information that are relevant to understanding of when earthquakes may occur. If viewed as complex stochastic time series, such data may be analyzed by methods that provide deeper insights into their nature, hence leading to better understanding of the data and their possible implications for earthquakes. In this paper, we provide further evidence for our recent proposal [P. Mansour *et al.*, *Phys. Rev. Lett.* **102**, 014101 (2009)] for the existence of a transition in the shape of the probability density function (PDF) of the successive detrended increments of the stochastic fluctuations of Earth's vertical velocity V_z , collected by broadband stations before moderate and large earthquakes. To demonstrate the transition, we carried out extensive analysis of the data for V_z for 12 earthquakes in several regions around the world, including the recent catastrophic one in Haiti. The analysis supports the hypothesis that before and near the time of an earthquake, the shape of the PDF undergoes significant and discernable changes, which can be characterized quantitatively. The typical time over which the PDF undergoes the transition is about 5–10 h prior to a moderate or large earthquake.

DOI: [10.1103/PhysRevE.82.036105](https://doi.org/10.1103/PhysRevE.82.036105)

PACS number(s): 89.75.Da, 05.45.Tp, 64.60.Ht, 91.30.Px

I. INTRODUCTION

A typical statement about earthquakes, especially the moderate and large ones, is that they are not predictable, because predicting earthquakes entails forecasting three parameters: when and where earthquakes occur, and what their magnitude M is. Predicting all the three parameters is clearly very difficult. This is despite the fact that there are many known precursors to impending earthquakes, ranging from peculiar behavior of animals, to thermal radiation from the earth. Despite the difficulty but also motivated by it, the past several decades have witnessed the development of several concepts and ideas for explaining various aspects of earthquakes [1]. They range from the Gutenberg-Richter law [2] for the number of earthquakes with a magnitude greater than a given value M , to the Omori law [3] for the distribution of the aftershocks, the Bak-Tang concept of self-organized criticality [4], the critical percolation backbone as the cluster that represents the spatial distribution of earthquakes [5–7], log-periodic corrections to the power law that describes the time dependence of the released energy as an earthquake is approached [8–10], and other concepts [1].

A main challenge is developing accurate methods for analyzing seismic data, in order to understand the precursors and

their implications for an impending earthquake, which may then be used for developing quantitative measures as alerts for earthquakes. There are currently a large number of stations around the world that carry out high quality measurements of seismic activities, and collect data for their various characteristics. Such data are usually viewed as examples of complex stochastic time series, and are analyzed by various methods [1]. Understanding the events that lead to large earthquakes entails having the ability to accurately analyze such time series and revealing their nature.

The analysis of seismic data may be facilitated if we recognize that they belong to a much larger class of stochastic time series, the analysis of which has been the subject of much research over the past several years. In particular, there has been much recent interest in investigating the precursors to, and the predictability, of extreme increments in time series in general [11]. At the same time, there has also been much interest in investigating the precursors to, and the predictability of, extreme increments in the time series associated with disparate phenomena, ranging from earthquakes [12,13], to epileptic seizures [14], and stock market crashes [15].

The goal of the present paper is to analyze high-quality data for eleven large earthquakes around the world by a method that has been developed for detecting extreme increments in stochastic time series, and to show that the analysis leads to deeper insights into occurrence of such earthquakes,

*moe@iran.usc.edu

and might provide the basis for developing an alert for them. Using the method, we reported in a recent Letter [16] the existence of a transition in the shape of the probability density function (PDF) of the detrended increments of the stochastic fluctuations [17] of Earth’s vertical velocity V_z , collected by broad-band stations. It was demonstrated that there is a well-defined transition from a Gaussian to a non-Gaussian PDF of the detrended increments as a moderate or large earthquake is approached. Depending on the magnitude of the earthquake, the typical time at which the PDF undergoes the transition before an earthquake is about 5–10 h. We also argued that, due to the attenuation of elastic waves [18–22], only the broadband stations that are close enough to the epicenters with distances $d \approx 300\text{--}500$ km are able to detect such a transition.

In the present paper, we continue the analysis that we began in our recent Letter [16] and report further extensive analysis of the data for V_z for ten other earthquakes around the world. The analysis provides further support for the existence of the transition in the earthquakes that we analyze. The earthquake that are analyzed occurred in Algeria, California (USA), China, Indonesia, Iran, Japan, Pakistan, Peru, Spain, and recent earthquakes in Italy and Haiti.

The rest of the paper is organized as follows. In Sec. II we describe briefly the data that we analyze and how they were obtained. Section III describes the method for the analysis of the data. In Sec. IV the results are presented and discussed. The last section provides a summary and outlines future directions in this problem.

II. DATA

The time series that represent the vertical velocity $V_z(t)$ of Earth are utilized in the analysis, because they provide the most unambiguous indication for the existence of the transition that we describe. The sampling rate of the data was 100 Hz, and for each earthquake we analyzed 8 640 000 data points. The data were obtained through the Inc. Research Institutions for Seismology (IRIS), which is a consortium of research universities dedicated to exploring the Earth’s interior through the collection and distribution of seismological data [23]. Two types of data are provided by the IRIS data management center, namely, continuous and event-related data. The former type of data are for those users that are interested in time windowing their own data. There are also archived data in the form of customized sets, defined by the user. Event-related data are available for those users who are interested in predefined event-oriented time windows [24]. The complete explanations for how to download data, and the tools that are necessary for doing so are given in Ref. [23].

III. ANALYSIS OF THE DATA

The data for $V_z(t)$ are first detrended in order to remove any possible trends in the time series, $x(t) \equiv V_z(t)$. To do so, $x(t)$ is divided into semi-overlapping subintervals $[1+s(k-1), s(k+1)]$ of length $2s$ and labeled by $k \geq 1$. $x(t)$ is then fitted to a third-order polynomial [16,25–28], in order to de-

trend the original series in the corresponding time window. The detrended increments on scale s are defined by, $Z_s(t) = x^*(t+s) - x^*(t)$, where $t \in [1+s(k-1), sk]$, with $x^*(t)$ being the detrended series, i.e., the deviation of $x(t)$ from its fitted value.

We then utilize a new approach, originally proposed for fully-developed turbulence [28–31], in order to describe the cascading process that determines how the fluctuations in the series evolve as one passes from one scale to another scale. For a fixed t , the fluctuations at scales s and λs are related through the cascading rule,

$$Z_{\lambda s}(t) = W_\lambda Z_s(t), \quad \forall s, \lambda > 0, \quad (1)$$

where $\ln(W_\lambda)$ is a random variable. Iterating Eq. (1) implicitly forces the random variable W_λ to follow a log infinitely-divisible law [32]. One of the simplest candidates for such processes is [26,27], $Z_s(t) = \zeta_s(t) \exp[\omega_s(t)]$, where ζ_s and $\omega_s(t)$ are independent Gaussian variables with zero mean and variances σ_ζ^2 and σ_ω^2 . The PDF of $Z_s(t)$ has fat tails that depend on the variance of ω_s , and is expressed by [31],

$$P_s(Z_s) = \int F_s\left(\frac{Z_s}{\sigma}\right) \frac{1}{\sigma} G_s(\ln \sigma) d \ln \sigma, \quad (2)$$

where F_s and G_s are both Gaussian distributions with zero mean and variances σ_s^2 and λ_s^2 , respectively. Thus, for example,

$$G_s(\ln \sigma) = \frac{1}{(\sqrt{2\pi\lambda_s})} \exp(-\ln^2 \sigma / 2\lambda_s^2).$$

In this case, $P_s(Z_s)$ is expressed by Eq. (2) and converges to a Gaussian distribution as $\lambda_s^2 \rightarrow 0$. Although Eq. (2) is equivalent to what is used in a log-normal cascade model for fully developed turbulence [33], it also describes approximately the non-Gaussian PDFs observed in such diverse phenomena and systems as the foreign exchange markets [26,34–36], and heartbeat interval fluctuations [35,37,38].

To carry out a quantitative analysis of the seismic times series, we focus on the deviations of the detrended increments’ PDF from a Gaussian distribution, and the dependence of the correlations in the increments on the scale parameter s . Consider the time series for an earthquake. We divide the series into two parts over two distinct time intervals:

- (i) data set (I)—the background fluctuations far from the event’s time, and
- (ii) data set (II) close (< 5 hours) to the earthquake.

To estimate the non-Gaussian parameter λ_s and its uncertainty using statistical inference in Eq. (2), we rely on a commonly utilized method, namely, the Bayesian statistics. We do not, however, have any prior estimate for the free parameter λ_s . Consequently, the Bayesian method reduces to the maximum likelihood analysis. Since all the measurements’ errors are essentially Gaussian, the maximum likelihood analysis reduces to the least-squares fitting [39], namely, the χ^2 method,

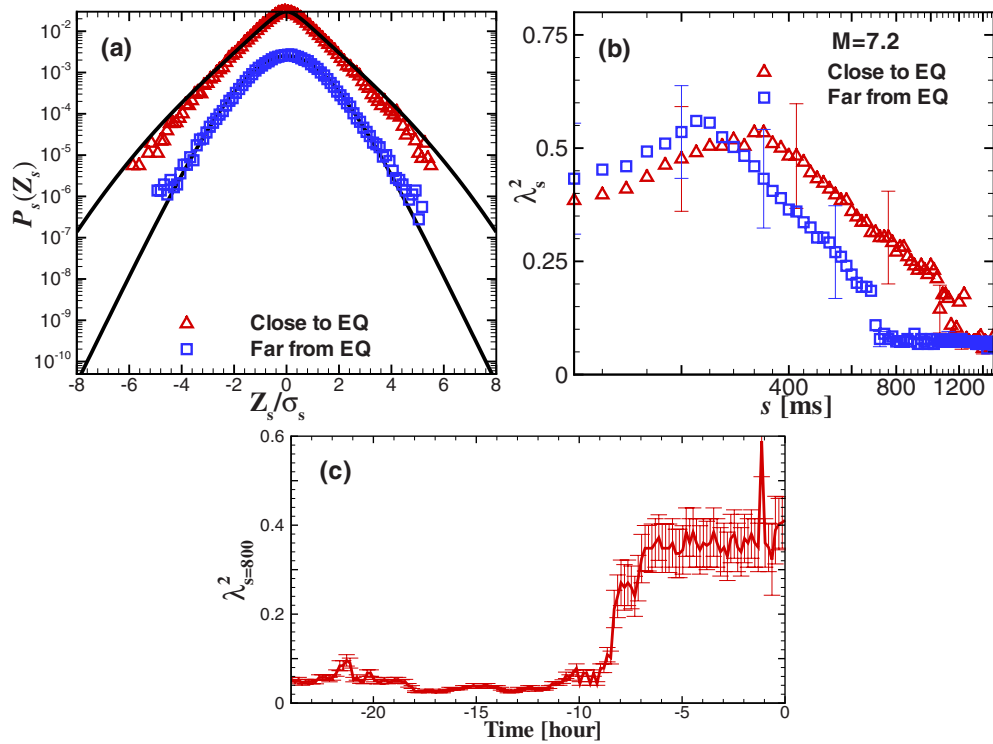


FIG. 1. (Color online) (a) The increments' PDFs for the $M=7.2$ event near south of coast of western Honshu, Japan, for $s=800$ ms, and for far from, and close to, the event. Solid curves are the PDFs based on the cascade model. (b) Scale-dependence of λ_s^2 versus $\log s$. (c) The local temporal dependence of λ_s^2 for $s=800$ ms, over a 1 h period, indicating a gradual, systematic increase as the earthquake approaches.

$$\chi^2(\lambda_s) = \int dz \frac{[P_s(z) - P_{\text{Castaing}}(z, \lambda_s)]^2}{[\sigma_{\text{Numeric}}^2(z) + \sigma_{\text{Castaing}}^2(z, \lambda_s)]}, \quad (3)$$

where $P_s(z)$ and $P_{\text{Castaing}}(z, \lambda_s)$ are the directly calculated PDFs from the time series $\{Z\}$, and using the Castaing equation, Eq. (2), respectively. σ_{Numeric} is the error for $P_s(z)$, while σ_{Castaing} is related to the PDF derived by the right side of Eq. (2). For a fixed s , we construct the time series $\{Z\}$ and vary λ_s to minimize $\chi^2(\lambda_s)$. The best estimate of λ_s corresponds to the global minimum of χ^2 .

To evaluate the confidence region for the free parameter of model for each s , we used the goodness of the fit method. It can be shown, assuming Gaussian statistics for χ^2 , that the confidence region for one free parameter is bounded by the value of χ^2 , such that $\chi^2(\lambda_s) = \chi_{\min}^2(\lambda_s^*) - \Delta\chi^2(\lambda_s)$, where $\Delta\chi^2(\lambda_s)$ is determined using the distribution of χ^2 for one degree of freedom. For example, in the region bounded by $\Delta\chi^2=1$, the probability of finding the real value of the free parameter is equal to 0.683, or an uncertainty of $1-\sigma$. Scanning this region we determine the uncertainty of λ_s at a $1-\sigma$ confidence level.

While we find an accurate parametrization of the PDFs by $\lambda_s^2(s)$ for both data sets, for all the data that we analyzed the deviation of $\lambda_s^2(s)$ from zero is a possible indicator of the non-Gaussian statistics. Moreover, in all the cases the PDF of Z_s for the data set (I) becomes essentially Gaussian as s increases to about 800 ms, whereas it deviates from the Gaussian distribution for the data set (II). The time scale $s=800$ ms for λ_s^2 within a moving window was estimated by

plotting λ_s^2 vs s for the data set (I) and selecting s such that $\lambda_s \rightarrow 0$ (see also below).

IV. RESULTS AND DISCUSSION

We first describe in detail the results for one earthquake, and then summarize the results for the rest of the earthquakes that we have analyzed. Thus, let us consider the data for the September 05, 2004, $M=7.2$ event that occurred in western Honshu, Japan. The data that were made available to us were from a station at a distance $d \approx 172$ km from the epicenter. If data from other stations with comparable distances from the epicenter are analyzed, we expect to obtain similar results. We consider the time series for Earth's vertical velocity corresponding to the event over two time intervals described above, namely, (i) data set I—the background fluctuations far from the event's time—and (ii) data set II close (<5 hours) to it. After detrending the data with third-order polynomials as described above, the PDF for the variable $Z_s(t)$ was constructed numerically. As shown in Fig. 1(a), the PDF of Z_s for the data set I is essentially Gaussian for $s=800$ ms, whereas it deviates significantly from the Gaussian distribution for the data set II.

Figure 1(a) also indicates that accurate parameterizations of the PDFs for both data sets (solid lines) were obtained, particularly within a factor 3 of the standard deviations. The scale-dependence of λ_s^2 is shown in Fig. 1(b). For the data set I and time scales $200 \text{ ms} < s < 600 \text{ ms}$ we find, $\lambda_s^2 \propto \log s$. For the data set II, on the other hand, the logarithmic regime extends to $400 \text{ ms} < s < 1000 \text{ ms}$. As pointed out earlier,

nonzero values of $\lambda_s^2(s)$ are a possible indicator of the non-Gaussian statistics [31,36]. We speculate that such anomalous behavior might be related to the noise generated by the cracks that presumably develop before the earthquake. Due to its significance, we believe that the speculation should be studied further.

The above analysis may provide a basis for developing a possible new precursor for detecting an impending earthquake. To explore the possibility, a window that contains one hour of the data was selected and moved with $\Delta t = 15$ minutes, in order to determine the temporal dependence of λ_s^2 . Guided by Fig. 1(b), the local temporal variations of λ_s^2 for $s=800$ ms were investigated. According to Fig. 1(b), for $s \approx 800$ ms, the difference between values of λ_s^2 for the background data I and the data set II near the earthquake is large and statistically significant. Hence, such a time scale may represent the characteristic time for the emergence of the dynamics of the non-Gaussian indicator λ_s^2 . As one may expect, the time scale $s \approx 800$ ms identified above is *not* universal and depends on the area, i.e., the geology of the rock.

Figure 1(c) displays well-pronounced, systematic increases in λ_s^2 as the earthquake is approached. Taking into account the estimated error of λ_s^2 for the background fluctuations in Fig. 1(c), we see that about $t_a=8$ hours before the earthquake, values of λ_s^2 are larger by more than two standard deviations than those computed for the background.

To test whether the same phenomenon exists in time series of other earthquakes, which would represent a test on the reliability of the hypothesis on the existence of the transition as an earthquake is approached, the same analysis was carried out for ten other earthquakes in various parts of the world. The results for are given in Fig. 2, where the local temporal dependence of λ_s^2 over a one hour period is shown. The earthquakes are represented by (M, D, d, P) , where D is the date of the event, d the distance (in km) of the station that collected the data from the epicenter, and P the place of the results in Fig. 2. The earthquakes analyzed are the (9,12/26/2004,330,A) event in Sumatra, Indonesia; (8,8/15/2007,158,B) near the coast of Peru; (7.9,5/12/2008,550,C) in Sichuan, China; (7.6,8/10/2005,525,D) in Pakistan, and the data for the same Pakistani earthquake but collected in a separate station at 550 km from the epicenter (E); (7,1/17/1995,480,F) near the south coast of western Honshu, Kobe, Japan; (6.8,10/23/2004,170,G) near the west coast of Honshu, Japan; (6.3,4/6/2009,308,H) in central Italy; (6.3,5/28/2004,77,I) in northern Iran, and the (4.7,1/19/2008,114,J) event in California (USA). In each case we analyzed the data that were available to us.

As Fig. 2 indicates, for all but the California event, one obtains clear and significant changes in the values of λ_s^2 , which might be interpreted as alert for the earthquakes. There is no discernible alert for the California earthquake, because its magnitude was small. More generally, we find that for the events with magnitudes $M \leq 5$ the increase in λ_s^2 is not large, even if the data are collected at stations as close as 100 km to the epicenters [16]. Thus, deeper understanding of the reason for the significant changes in the value of λ_s^2 as a moderate or large earthquake is approached may lead to the development of a meaningful and reliable alert for earthquakes with magnitude $M > 5$.

Clearly, it would be highly desirable to test this proposal further by analyzing the data for many more moderate and large earthquakes around the world. We also note that, due to the attenuation of elastic waves in the Earth's crust [18–22], stations that are too far from an earthquake's epicenter cannot provide an accurate estimate for the change in the value of λ_s^2 and, therefore, would not be able to be used as an alert for earthquakes. This assertion was checked for several earthquakes by analyzing the data from stations that were too far from the epicenters. For large earthquake, however, we observe that even the stations with a distance $d \approx 500$ km from the epicenters provide an accurate estimate of the change in the value of λ_s^2 for an impending earthquake; see Fig. 2.

The importance of the results shown in Figs. 1 and 2 is that, they indicate that the increments' PDFs for large s ms are essentially Gaussian, i.e., $\lambda_s^2 \rightarrow 0$ [for the data set (II)]. For example, for the $M=7.2$ earthquake analyzed in Fig. 1, we obtain a Gaussian PDF for $s > 2000$ ms. Thus, if we transform the time scale to a length scale via the velocity of elastic waves in Earth, ~ 5000 m/sec, the corresponding length scale is about 10 km, implying that larger earthquakes have larger characteristic length scales, and that for the smaller events the active part of the fault is smaller. As one moves down the cascade process from large to small scales, one expects the statistics to increasingly deviate from Gaussianity, in order to arrive at Eq. (2). Note that, a non-Gaussian PDF with fat tails on small scales indicates a higher probability of occurrence of short-time *extreme* seismic fluctuations.

From the point of view of the increments' PDF, the non-Gaussian noise with uncorrelated ω_s in the process, $Z_s(t) = \zeta_s(t) \exp[\omega_s(t)]$, and a multifractal formulation are indistinguishable, because their one-point statistics at any given scale may be identical. Thus, to understand the origin of the non-Gaussian fluctuations, we also used an alternative method for studying the correlation functions of the local fluctuations [30]. The magnitude of the local variance over a scale s is defined by, $\sigma_s^2(t) = n_s^{-1} \sum_{k=-n_s/2}^{n_s/2} Z_s(t+k\Delta t)^2$, and, $\bar{\omega}_s(i) = \frac{1}{2} \log \sigma_s^2(i)$. Here, Δt is the sampling interval and, $n_s \equiv s/\Delta t$. The magnitude of the correlation function of $\bar{\omega}_s$ is then defined by

$$C^{(s)}(\tau) = \langle [\bar{\omega}_s(t) - \langle \bar{\omega}_s \rangle][\bar{\omega}_s(t + \tau) - \langle \bar{\omega}_s \rangle] \rangle, \quad (4)$$

where $\langle \cdot \rangle$ indicates a statistical average. Figure 3 presents the results for the earthquakes analyzed in Fig. 2. The correlation function decays sharply for the data set (I)—far from the earthquakes—whereas it is of the long-range type for the set (II) close to the earthquakes, where the PDF deviates from being Gaussian even for $s > 800$ ms. Although one can argue that the deviations might be due to an underlying Lévy statistics, this possibility can be safely ruled out, due to the

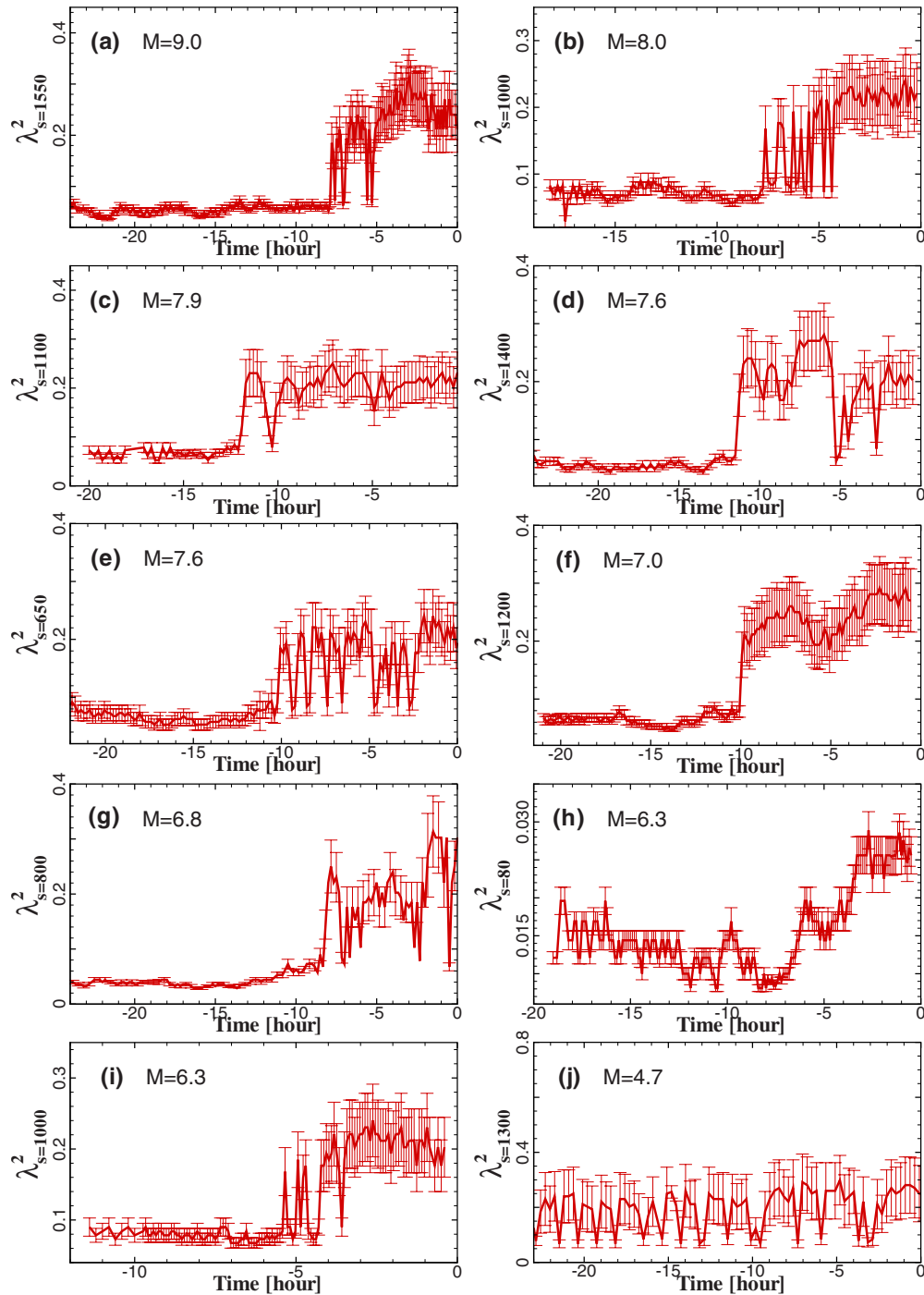


FIG. 2. (Color online) Time-dependence of the non-Gaussian parameter λ_s^2 for the 9 earthquakes that were analyzed. See the text for the location and date of the events.

deduced hierarchical structures that imply that the increments for different scales are *not* independent.

As mentioned earlier, due to the attenuation and localization of elastic waves in rock, the stations that are far from an earthquake epicenter cannot provide any clue to the transition to a non-Gaussian PDF and significant changes in the value of the parameter λ_s^2 . We checked the assertion for several earthquakes. For example, when we analyzed the data for the $M=5.4$ earthquake in California that occurred at (40.837 N, 123.499 W) on April 30, 2008, and collected at a

station at a distance $d \approx 128$ km from the epicenter, the change in the value of λ_s^2 occurred 3 h before the earthquake, whereas the data that had been recorded at a station with $d \approx 400$ km did not provide any clue to the transition to a non-Gaussian PDF of the increment and significant change in the value of λ_s^2 . Similarly, we analyzed the data for the $M=6$ earthquake in Nevada that occurred on February 21, 2008. The online data belong to the PAH station from NN and KEB, KBO, KHMB, KCPB, and KRMB stations in the NC network. The distance of the stations from the earth-

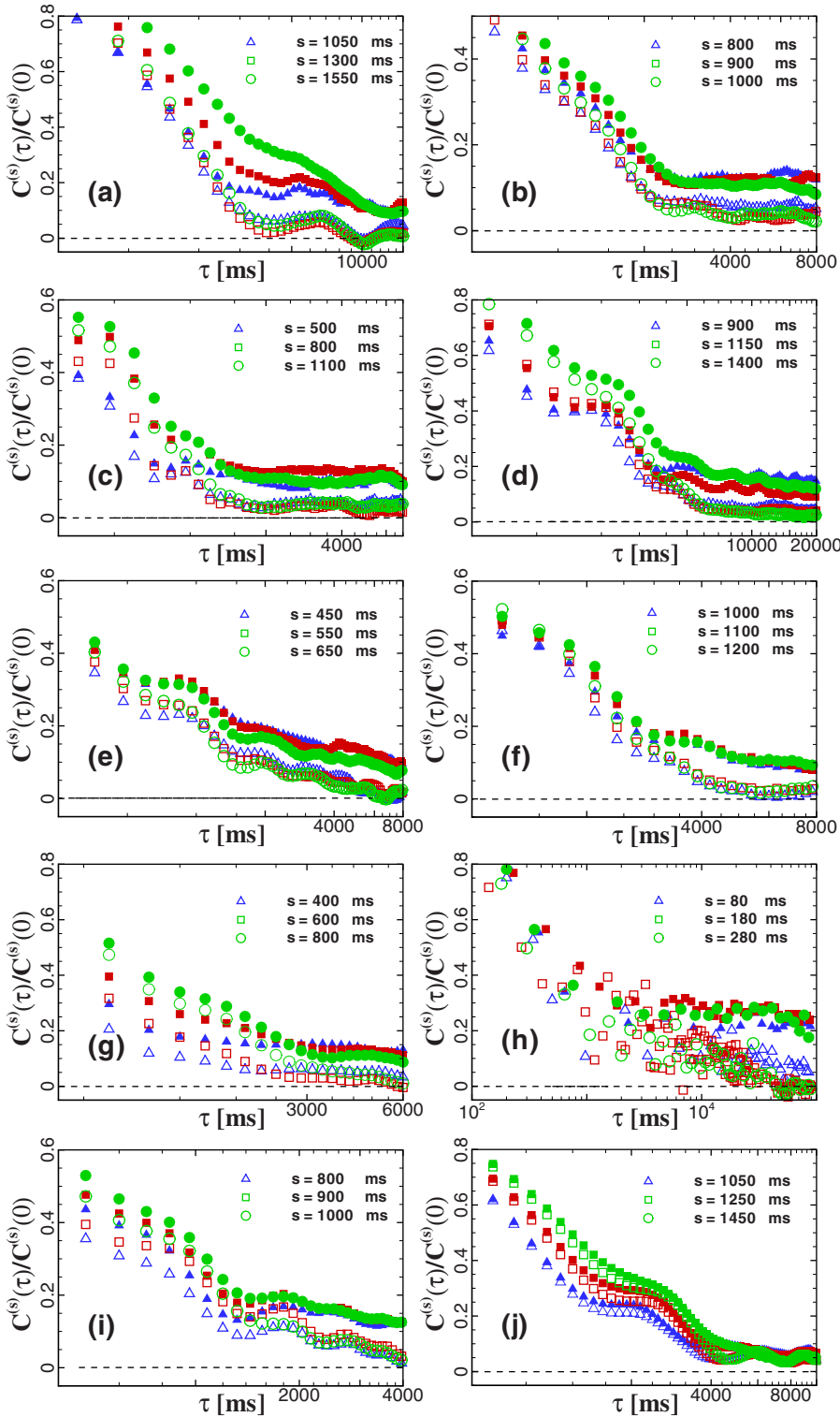


FIG. 3. (Color online) The correlation functions $C^{(s)}(\tau)$ for the 9 earthquakes that are analyzed in Fig. 2. See the text for the location and date of the events.

quake epicenter were all around 450 km, too far to detect any transition, due to the localization of elastic waves. As a result, no discernable changes were obtained.

After completion of the paper, a devastating earthquake of magnitude $M=7.0$ occurred in Haiti at (18.457N,72.533W) on Tuesday January 12, 2010. Thus, to further test the new method of analysis of the data and its implications for earthquakes, we analyzed the available broadband data for the Haiti earthquake obtained from the stations SDDR in Presa

de Sabenta in the Dominican Republic, from the Caribbean Network (operated by the United States Geological Surveys) at a location with latitude 18.98, longitude -71.29 , and elevation 589 m. The distance of the station to the epicenter is about 165 km.

Figure 4 shows the continuous deformation of the increments' PDFs for the Haiti earthquake for times that are far from, and close, to the event, and compares the PDFs based on Eq. (2) with the Gaussian PDF. As Fig. 4 indicates, the fit

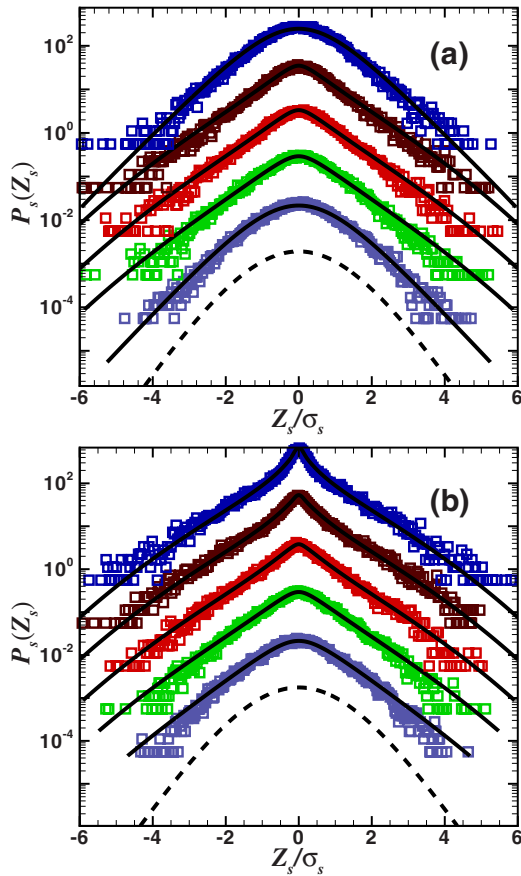


FIG. 4. (Color online) Continuous deformation of the increments' PDFs for the 2010 Haiti earthquake for, from top to bottom, $s=250, 500, 750, 1000, 1250$ ms, and (a) far from, and (b) close to the earthquake. The solid curves are the PDFs based on Eq. (2), while the dashed curves are the Gaussian PDF.

to Eq. (2) is very accurate. Figure 5 demonstrates how the parameter λ_s^2 varies with the time scale s , both close to the earthquake and away from it. In the former case λ_s^2 achieves its maximum value around $s=25$ ms, and then sharply decreases. Thus, we studied the variations of $\lambda_{s=250}^2$ versus time

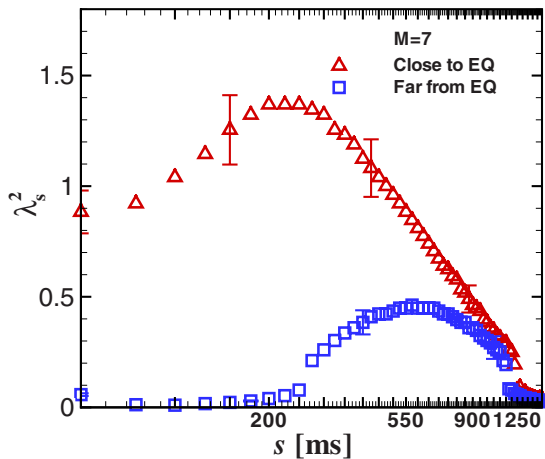


FIG. 5. (Color online) Dependence of the non-Gaussian parameter λ_s^2 on the time scale s , both close to the earthquake and away from it. The results are for the 2010 Haiti earthquake.

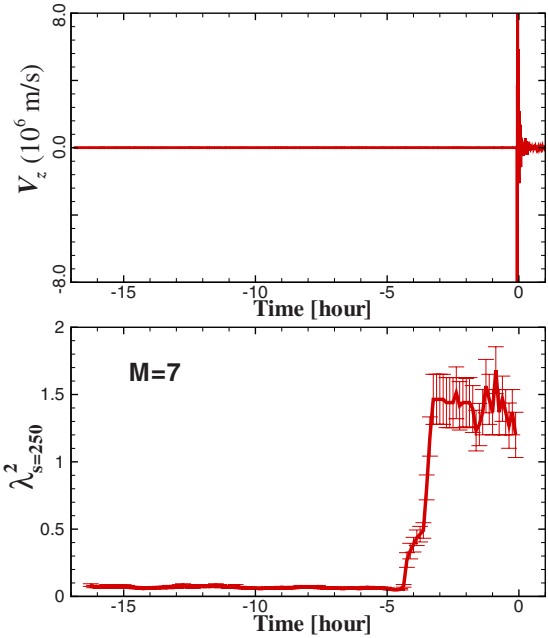


FIG. 6. (Color online) Dependence of $\lambda_{s=250}^2$ (see Fig. 5) of the time as the Haiti earthquake is approached. The results indicate that 5 h before the earthquake the value of $\lambda_{s=250}^2$ suddenly increases, hence signaling the transition in the PDF. On the scale of the figure the velocity appears flat, but its fluctuations can be seen on a more refine horizontal axis.

as the earthquake was approaching. The results are presented in Fig. 6, which presents the local temporal dependence of λ_s^2 for $s=250$ ms for the earthquake along with the vertical velocity of Earth. Figure 6 indicates a gradual, systematic increase in λ_s^2 on approaching the earthquake. Five hours before the earthquake the value of the parameter suddenly increases, hence signaling that an earthquake is going to occur.

A reliable and credible earthquake precursor should not provide any false alarm or, at least, the number of the false alarms that it predicts should be small. In our analysis, the alarms are accepted if at least two, and preferably three, independent stations indicate the same. Otherwise, the alarm is not accepted. In fact, one station might, by itself, provide a false indication for the transition from the Gaussian to non-Gaussian distribution and, hence, an alarm. But, that is not accepted unless at least one other station at a comparable distance, which is typically around 300 km, indicates the same.

V. SUMMARY

A method for analyzing seismic data was presented, and was used to analyze the time series that represent Earth's vertical velocity, collected at the broadband stations near the epicenters of earthquakes. The analysis is based on detrending the data, and then studying the probability density function of the successive increments of the detrended data, both near and away from an earthquake. The time scale s for moving the window that is used to analyze the detrended

data close and away from an earthquake is estimated by a plot of the non-Gaussian parameter λ_s^2 versus s for the data set (I) far from the earthquake, and selecting s such that $\lambda_s^2 \rightarrow 0$. The last step of the method consists of estimating λ_s^2 in some windows (here, in windows of about 15 min) and moving it along the time series, in order to obtain the variations of λ_s^2 with t . We showed that the PDF of the increments undergoes a transition from a Gaussian to a non-Gaussian distribution, and that the difference between λ_s^2 for data sets (I) (far from the earthquake) and (II) (close to earthquake) is statistically significant. The same trends were also shown to exist in the temporal correlation function.

Therefore, the analysis provides a consistent picture of what happens as a moderate or large earthquake is approached. The PDF of the detrended increments undergoes a transition from Gaussian to non-Gaussian, while at the same time the correlation function changes from a sharply decaying function for the data set (I) (far from the earthquake) to one of a long-range type for the data set (II) close to the earthquake. The non-Gaussian parameter λ_s^2 (and the flatness parameter of the PDF [16]) depends on the time, but as an

earthquake is approached, its magnitude changes suddenly.

Clearly, it is too early to claim that the transition to a non-Gaussian PDF, and the significant change in the value of the parameter λ_s^2 that occurs at the transition point, provide accurate and timely alarms for all impending moderate and large earthquakes, free of any false alarm. Indeed, we make no such claims, but only report on the transition and the change in the value of λ_s^2 . One must analyze a large amount of data *online* from many stations, in order to estimate the percentage of possible false alarms. We have begun doing so for the online data (as they come in real time) in 40 stations in Spain. In any case, what the present analysis indicates is, in our opinion, significant enough to be studied further.

ACKNOWLEDGMENTS

We thank the various organizations around the world that provided us with the data. M.R.R.T. thanks the Alexander von Humboldt Foundation and the Knowledge Archive for financial support.

-
- [1] *Modelling Critical and Catastrophic Phenomena in Geoscience, A Statistical Physics Approach*, Lecture Notes in Physics Vol. 705, edited by P. Bhattacharyya and B. K. Chakrabarti (Springer, Berlin, 2006).
- [2] B. Gutenberg and R. F. Richter, *Seismicity of the Earth* (Hafner, New York, 1965).
- [3] T. Utsu, Y. Ogata, and R. S. Matsu'ura, *J. Phys. Earth* **43**, 1 (1995).
- [4] P. Bak and C. Tang, *J. Geophys. Res.* **94**, 15635 (1989).
- [5] M. Sahimi, M. C. Robertson, and C. G. Sammis, *Phys. Rev. Lett.* **70**, 2186 (1993).
- [6] H. Nakanishi, M. Sahimi, M. C. Robertson, C. G. Sammis, and M. D. Rintoul, *J. Phys. I* **3**, 733 (1993).
- [7] M. C. Robertson, C. G. Sammis, M. Sahimi, and A. J. Martin, *J. Geophys. Res. B* **100**, 609 (1995).
- [8] D. Sornette and C. G. Sammis, *J. Phys. I* **5**, 607 (1995).
- [9] M. Sahimi and S. Arbabi, *Phys. Rev. Lett.* **77**, 3689 (1996).
- [10] D. Sornette, *Phys. Rep.* **297**, 239 (1998).
- [11] S. Hallerberg and H. Kantz, *Phys. Rev. E* **77**, 011108 (2008).
- [12] D. D. Jackson, *Proc. Natl. Acad. Sci. U.S.A.* **93**, 3772 (1996).
- [13] M. R. Rahimi Tabar, M. Sahimi, F. Ghasemi, K. Kaviani, M. Allamehzadeh, J. Peinke, M. Mokhtari, M. Vesaghi, M. D. Niry, A. Bahraminasab, S. Tabatabai, S. Fayazbakhsh, and M. Akbari, in Ref. [1], p. 281.
- [14] F. Mormann, T. Kreuz, C. Rieke, R. G. Andrzejak, A. Kraskov, P. David, C. C. Elger, and K. Lehnertz, *Clin. Neurophysiol.* **116**, 569 (2005).
- [15] D. Sornette, *Why Stock Markets Crash* (Princeton University Press, Princeton, 2003).
- [16] P. Manshour, S. Saberi, M. Sahimi, J. Peinke, A. F. Pacheco, and M. R. Rahimi Tabar, *Phys. Rev. Lett.* **102**, 014101 (2009).
- [17] N. M. Shapiro, M. Campillo, L. Stehly, and M. H. Ritzwoller, *Science* **307**, 1615 (2005).
- [18] F. Shahbazi, A. Bahraminasab, S. M. Vaez Allaei, M. Sahimi, and M. R. Rahimi Tabar, *Phys. Rev. Lett.* **94**, 165505 (2005).
- [19] S. M. Vaez Allaei and M. Sahimi, *Phys. Rev. Lett.* **96**, 075507 (2006).
- [20] A. Bahraminasab, S. M. Vaez Allaei, F. Shahbazi, M. Sahimi, M. D. Niry, and M. R. Rahimi Tabar, *Phys. Rev. B* **75**, 064301 (2007).
- [21] R. Sepehrinia, A. Bahraminasab, M. Sahimi, and M. R. Rahimi Tabar, *Phys. Rev. B* **77**, 014203 (2008).
- [22] E. Larose, L. Margerin, B. A. van Tiggelen, and M. Campillo, *Phys. Rev. Lett.* **93**, 048501 (2004).
- [23] See, <http://www.iris.edu/>. How to access the data is described at <http://www.iris.org/data/tutorial.htm/newline>. The request for obtaining the tools that are needed for downloading the data should be made at <http://www.iris.org/data/wizard/tool.htm>.
- [24] K. Kiyono, Z. R. Struzik, N. Aoyagi, S. Sakata, J. Hayano, and Y. Yamamoto, *Phys. Rev. Lett.* **93**, 178103 (2004).
- [25] K. Kiyono, Z. R. Struzik, N. Aoyagi, F. Togo, and Y. Yamamoto, *Phys. Rev. Lett.* **95**, 058101 (2005).
- [26] K. Kiyono, Z. R. Struzik, and Y. Yamamoto, *Phys. Rev. Lett.* **96**, 068701 (2006).
- [27] G. R. Jafari, M. S. Movahed, P. Noruzzadeh, A. Bahraminasab, M. Sahimi, F. Ghasemi, and M. R. Rahimi Tabar, *Int. J. Mod. Phys. C* **18**, 1689 (2007).
- [28] U. Frisch and D. Sornette, *J. Phys. I* **7**, 1155 (1997).
- [29] J. F. Muzy, J. Delour, and E. Bacry, *Eur. Phys. J. B* **17**, 537 (2000).
- [30] A. Arneodo, E. Bacry, S. Manneville, and J. F. Muzy, *Phys. Rev. Lett.* **80**, 708 (1998).
- [31] B. Castaing, Y. Gagne, and E. J. Hopfinger, *Physica D* **46**, 177 (1990).
- [32] B. Dubrulle, *Phys. Rev. Lett.* **73**, 959 (1994).
- [33] B. Chabaud, A. Naert, J. Peinke, F. Chilla, B. Castaing, and B. Hebral, *Phys. Rev. Lett.* **73**, 3227 (1994).

- [34] H. E. Stanley and V. Plerou, *Quant. Finance* **1**, 563 (2001).
- [35] P. A. Varotsos, N. V. Sarlis, H. K. Tanaka, and E. S. Skordas, *Phys. Rev. E* **72**, 041103 (2005).
- [36] S. Ghashghaie, W. Breymann, J. Peinke, P. Talkner, and Y. Dodge, *Nature (London)* **381**, 767 (1996).
- [37] M. De Menech and A. L. Stella, *Physica A* **309**, 289 (2002).
- [38] F. Caruso, A. Pluchino, V. Latora, S. Vinciguerra, and A. Rapisarda, *Phys. Rev. E* **75**, 055101(R) (2007).
- [39] P. E. Greenwood and M. S. Nikulin, *A Guide to Chi-Squared Testing* (Wiley, New York, 1996).